AC SUSCEPTIBILITY MEASUREMENT OF SM DOPED Bi(Pb)SrCaCuO

by

ERGÜN KÜÇÜK

THESIS SUBMITTED TO

THE GRADUATE SCHOOL OF NATURAL AND APPLIED SCIENCES

OF

THE ABANT İZZET BAYSAL UNIVERSITY

IN PARTIAL FULFILLMENT OF THE REQUIREMENTS FOR THE DEGREE

OF

MASTER OF SCIENCE

IN

THE DEPARTMENT OF PHYSICS

August 2005

Approval of the Graduate School of Natural and Applied Science

Prof. Dr. Davut KÖŞKER

Director

I certify that this thesis satisfies all the requirements as a thesis for the degree of Master of Science.

Prof. Dr. Ahmet Turan ALAN

Head of Physics Department

This is to certify that we have read this thesis and that in our opinion it is fully adequate, in scope and quality as a thesis for the degree of Master of Science.

Assoc.Prof.Dr.Ahmet VARİLCİ

Supervisor

Examining Committee Members

1. Assoc.Prof. Dr. Ahmet VARİLCİ ………………………….....
2. Assoc. Prof. Dr. Resul ERYİĞİT .... ……….…………
3. Assist. Prof. Dr. Cabir TERZİOĞLU …………………………..

ABSTRACT

AC SUSCEPTIBILITY MEASUREMENT OF SM DOPED Bi(Pb)SrCaCuO

ERGÜN KÜÇÜK

Master of Science, Department of Physics

Supervisor: Assoc. Prof. Dr Ahmet VARİLCİ

August, 2005, [52] pages

In this thesis, after investigating the general historical development of high temperature superconductors, the design of AC susceptometer was made. After design, we studied on AC characteristic of $Bi_{1.6}Pb_{0.4}Sr_2Ca_{2-x}Sm_xCu_3O_y$ with Sm substitution for (x=0, x=0.0005 x=0.001 x=0.005). We obtained imaginary and real date by using home-made AC susceptometer. Critical current density $\boldsymbol{J_c}$ versus critical temperature $\boldsymbol{T_c}$ behaviour studied by using Bean Model and it seem that critical temperature of sample $Bi_{1.6}Pb_{0.4}Sr_2Ca_{2-x}Sm_xCu_3O_y$ with Sm substitution is decreasing with increasing of Sm substitution and critical current of sample $Bi_{1.6}Pb_{0.4}Sr_2Ca_{2-x}Sm_xCu_3O_y$ is decreasing with increasing of Sm substitution. At that critical current decreasing was seen at first substitution. The decreasing at critical current was not as sharp as first substitution.

Keywords: Superconductivity, Resistivity, intergrain critical current density, AC magnetic susceptibility, magnetic flux, Bi(Pb)SrCaCuO

ÖZET

SM KATKILI Bi(Pb)SrCaCuO'NIN MANYETİK ALINGANLIK ÖLÇÜMLERİ

ERGÜN KÜÇÜK

Yüksek Lisans, Fizik Bölümü
Tez Danışmanı: Doç. Dr Ahmet Varilci

Ağustos 2005, [52] sayfa

Bu tezde, yüksek sıcaklık superiletkenlerinin tarihsel gelişimi incelendi, sonra AC susceptometerin dizaynı yapıldı, daha sonra ise (x=0 x=0.005 x=0.001 x=0.0005) için Sm katkılı $Bi_{1.6}Pb_{0.4}Sr_2Ca_{2-x}Sm_xCu_3O_y$ süperiletken numunenin AC manyetik alınganlığı çalışıldı. El yapımı AC susceptometeri kullanılarak bu numunenin süperiletken durumdaki gerçel ve sanal davranışları incelendi.

Kritik akım yoğunluğu, $\boldsymbol{J_c}$, ve kritik geçiş sıcaklığı, $\boldsymbol{T_c}$, davranışı Bean Modeli kullanarak çalışıldı ve görüldü ki numenin kritik sıcaklıgı Sm katkısının artışı ile azalmaktadır. Sm katkısındaki artışa karşılık kritik akım yoğunluğu da azalmaktadır, bu kritik akım yoğunlundaki azalış ilk katkılanmada çok belirgin olmaktadır.

Anahtar Kelimeler: **:** Süperiletkenlik, Direnç, Taneler Arası Kritik Akım Yoğunluğu, AC Manyetik Duygunluk, Manyetik Akı , Bi(Pb)SrCaCuO

To my family

ACKNOWLEDGMENTS

It is a great pleasure to thank many people who have contributed to the completion of this thesis through their knowledge, guidance, support and friendship. First of all, I would like to thank my thesis supervisor, Assoc Prof. Dr Ahmet Varilci for his support, guidance, patience and encouragement during the preparation of this thesis. I also, thank to Assist. Prof. Dr. Cabir Terzioğlu

I would like to thank all my teachers for their kind help, especially, Res.Assist. Dinçer Yeğen and Özgür Öztürk.

I want to thank specially to Dr. Mustafa Yılmazlar to prepare samples at Kirikkale University

TABLE OF CONTENTS

LIST OF TABLES

LIST OF FIGURES

Figures **Page**

CHAPTER 1

INTRODUCTION

Superconductivity is the name given to a remarkable combination of electric and magnetic properties that appears in certain metals when they are cooled to extremely low temperatures.

Such very low temperature first becomes available in 1908 when Kamerling Onnes at the University of the Leiden succeeded in liquefying helium. It had been known for many years that the resistance of the metals falls when they are cooled to a certain temperature. But it was not know what limiting value. Onnes measured the resistance of pure mercury and he discovered that the resistivity of pure mercury that absolutely disappears at temperature below about 4K [1]. The temperature at which the transition takes place is called the critical temperature, T_c. Onnes surmised correctly that he was dealing with a new state of matter below the critical temperature and coined the term superconductivity. This zero resistivity (or infinite conductivity) is known as superconductivity. It was later discovered that superconductivity could be destroyed (i.e. electrical resistance restored) if a sufficiently strong magnetic field were applied, and subsequently it was found that a metals in a superconducting state has very extraordinary magnetic properties, quite unlike those known at ordinary temperatures [1]. For many years it was thought that all superconductors behaved according to a basically similar pattern, however, it is now realized that there are two kinds of superconductors, which are known as Type-I and Type-II. The two types have many properties common but show considerable differences in their magnetic behaviors. These differences are sufficient for us to threat the two types separately. This phenomenon of superconductivity is vast potential important in technology because it would be very useful to be able to cause charge to flows thorough a superconductor without the thermal energy loses. Currents created in a superconducting ring, for example, have resisted for several many years without diminutions the electrons making up current require a force and a source of energy at start-up time, but not thereafter.

The London penetration depth that was discovered in 1938 this is how deep, in the metal, magnetic field lines can go and the metal will still superconductor. In 1957 John Bardeen, Leon Cooper, and John Schrieffer made the first theory of why things superconductor. This was called the BSC theory [2].

First high temperature superconductor was found in 1986. This sample was superconductor at a much higher temperature than the previous ones. In 1986, a truly breakthrough discovery was made in the field of superconductivity. Alex Müller and Georg Bednorz (above), researchers at the IBM Research Laboratory in Rüschlikon, Switzerland, created a brittle ceramic compound that becoming superconductor at the highest temperature known 30 K. What made this discovery so remarkable was that ceramics are normally insulators. They don't conduct electricity well at all. So, researchers had not considered them as possible high-temperature superconductor candidates. The Lanthanum, Barium, Copper and Oxygen compound that Müller and Bednorz synthesized, behaved in a not-as-yet-understood way. The discovery of this first of the superconducting copper-oxides (cuprates) won the 2 men a Nobel Prize the following year. It was later found that tiny amounts of this material were actually superconducting at 58 K, due to a small amount of lead having been added as a calibration standard making the discovery even more noteworthy.

In January of the 1987 a research team at the University of Alabama-Huntsville substituted Yttrium for Lanthanum in the Müller and Bednorz molecule and achieved an incredible 92 K $\boldsymbol{T_c}$ (critical temperature). For the first time a material today referred to as YBCO had been found that becoming superconductor at temperature warmer that liquid nitrogen a commonly available coolant.

In 1987, a new chain is added to superconductivity studies. Michael found the superconductivity in Bi-Sr-Cu-O system. In 1998, Medea and his group observed superconductivity at 105 K by adding calcium to this system as Bi-Sr-Ca-Cu-O. Also Tokana and his group found a stable at 101 K by adding lead to system. Addition of lead increases the ratio of the phase that has high critical temperature. Quidwai and his group observed the transition to superconductivity at 130-140 K by adding antimony to system.

In 1988, Sheng and Parkin observed superconductivity in Tl-Ba-Ca-Cu-O compound first at 110 K and then at 125 K. But this compound has cancerogenic effect and was not stable and it has to be produced each time. During these passing years, studies on different samples went on. In 1993 Schilling and his group observed superconductivity in $HgBa_2CaCu_3O_{1+x}$ compound at 133 K and Chu and his group observed superconductivity in high pressure with Hg based compound at 150K

CHAPTER 2

ELECTRICAL AND MAGNETIC PROPERTIES OF SUPERCONDUCTOR

2.1 Electrical Properties

2.1.1 Zero Resistance and Critical Temperature

The electrical resistivity of all metals and alloys decreases when they are cooled. The resistivity of a superconductor vanishes abruptly at a certain temperature. The temperature at which superconductors lose resistance is called transition temperature or critical temperature T_c. Below T_c; it enters an entirely different superconducting state. Superconducting transition is reversible: when they heated it recovered its normal resistivity at the temperature T_c. At the temperature above absolute zero the atoms are vibrated and will be displaced by various amounts of from their equilibrium position furthermore foreign atoms or other defects randomly distributed can interrupt the perfect periodicity. Both the thermals vibrations and any impurities or imperfections scatter the moving electrons and give rise to electrical resistance. When the temperature is lowered, the thermal vibrations of the atoms decrease and the conduction electrons are less frequently scattered. Any real specimens of metals cannot be perfectly pure and will contain some impurity. Therefore the electrons, in additions to being scattered by thermal vibrations of the lattice are scattered by impurities

2.1.2 AC Resistivity

Zero resistance in a superconducting metal means that there is no voltage drop along the specimen when a current is passed through, and by consequence no power is dissipated. This is, however, strictly true only for a DC current of constant value.

The appearance of resistance when AC current is applied can be explained if one makes the assumption that below the T_c the electrons in the superconductor can be divided into two categories: "superelectrons" which form so-called Cooper Pairs and carry electricity without resistance and the rest behaving like "normal" electrons, which scatter and when passing through the metal lattice experience resistance [3].

In the case of constant DC current, there must be no electric field present in the specimen; otherwise the superelectrons would accelerate continuously and the current would increase. In this case, there is no electromotive force to drive the normal electrons and all the current is lead through by the superelectrons, so no power dissipation appears at all.

In AC current, an electric field must be present to accelerate the electrons. Because of the inertial mass of the electrons (even if of very small magnitude), the supercurrent lags behind the electric field. Hence the superelectrons present inductive impedance. In addition, due to the presence of electric field, the normal electrons will carry some current, so that in overall the AC current will cause some power dissipation in a superconducting specimen.

2.2 Magnetic Properties

Each electron in an atom has orbital magnetic dipole moment and spin magnetic dipole moment that combine vectorially. The resultant of two vectors combines vectorially with similar resultants for all other electrons in the atoms. And the resultants for each atom combine with those for all other atoms in a sample or the materials. If the combination of all these magnetic dipole moments produces a magnetic field, then the materials are magnetic. There are three general type of magnetism: diamagnetism, paramagnetism and ferromagnetism.

The magnetic moments of free atoms have three principal sources, the spin with which electrons are endowed, their orbital angular momentum about nucleus, and the change in the orbital moments induced by an applied magnetic fields.

The first two effects give paramagnetic contributions to the magnetization, and the third gives a diamagnetic contributions. Atoms with filled electrons shells have zero spin and zero orbital moments: these moments are associated with unfilled shells. The magnetization M is defined as the magnetic moments per unit volume. **The magnetic susceptibity per unit volume** is defined as

$$\chi = M/H$$

Where H is applied magnetic field. The proportionality constant χ is being known as the magnetic susceptibility of the medium. In both systems of units χ is dimensionless.

Materials may be grouped into three magnetic classes, depending on the sign and magnitude of the susceptibility. Those materials for which χ is positive that is for which ***M*** is parallel to ***H*** are known as paramagnetic, whereas those for which χ is negative that is, for which ***M*** is opposite to ***H*** are diamagnetic. Table 2.1 gives susceptibilities for some representative substances, and emphasizes once more the smallness of the magnitude of χ .

Table 2.1: Magnetic susceptibilities of some materials

Material	χ(per cm^{-3})
Paramagnetic	
Al	$+2.2x10^{-5}$
Mn	$+98$
W	$+36$
Diamagnetism	
Cu	$-1.0x10^{-5}$
Au	-3.6
Hg	-3.2
Water	-9.0

2.2.1 Paramagnetic Materials

The spins/dipoles tend to align in parallel to an external magnetic field, an effect called paramagnetism. The best-known examples of paramagnetic materials are the ions of transition and rare-earth ions. The fact that these ions have incomplete atomic shells is what is responsible for their paramagnetic behavior. Paramagnetism is the tendency of the atomic magnetic dipoles, due to quantum-mechanical spin, in a material that is otherwise non-magnetic to align with an external magnetic field. This alignment of the atomic dipoles with the magnetic field tends to strengthen it, and is described by a relative magnetic permeability greater than unity (or, equivalently, a small positive magnetic susceptibility). In pure paramagnetism, the field acts on each atomic dipole independently and there are no interactions between individual atomic dipoles. Such paramagnetic behavior can also be observed in ferromagnetic materials that are above their Curie temperature. Paramagnetic materials attract and repel like normal magnets when subject to a magnetic field. Under relatively low magnetic field saturation when the majority of the atomic dipoles are not aligned with the field, paramagnetic materials exhibit magnetization according to Curie's Law:

$$M = C\frac{B}{T}$$

where $\boldsymbol{M}$ is the resulting magnetization, $\boldsymbol{B}$ is the magnetic flux density of the applied field, $\boldsymbol{T}$ is absolute temperature measured in and C is a material-specific Curie constant. This law indicates that paramagnetic materials tend to become increasingly magnetic, as the applied magnetic field is increased, but less magnetic as temperature is increased. Curie's law is incomplete because it fails to predict what will happen when most of the little magnets are aligned so Curie constant really should be expressed as a function of how much of the material is already aligned. Paramagnetic materials in magnetic fields will act like magnets but when the field is removed, thermal motion will quickly disrupt the magnetic alignment. In general paramagnetic effects are small (magnetic susceptibility of the order of 10^{-3} to 10^{-5}). Ferromagnetic materials above the Curie temperature become paramagnetic.

2.2.2 Ferromagnetic Materials

The property of ferromagnetism is due to the direct influence of two effects: spin and the Pauli Exclusion Principle. The spin of an electron has a magnetic dipole moment and creates a magnetic field. In many materials (specifically those with a filled electron shell), however, the electrons come in pairs of opposite spin, which cancel one another's dipole moments. Only atoms with unpaired electrons (partially filled shells) can experience a net magnetic moment from spin. A ferromagnetic material has many such electrons, and if they are aligned they create a measurable macroscopic field. Ferromagnetism involves an additional phenomenon, however: the spins tend to align spontaneously, without any applied field. This is a purely quantum-mechanical effect. Thus, an ordinary piece of iron generally has little or no net magnetic moment. However, if it is placed in a strong enough external magnetic field, the domains will re-orient in parallel with that field, and will remain re-oriented when the field is turned off, thus creating a “permanent" magnet. The net magnetization can be destroyed by heating and then cooling (annealing*)* the material without an external field. However, the magnetic susceptibility of ferromagnetic materials may be very large ($10^5 cm^{-3}$) and ferromagnetic substance becomes spontaneously magnetized below a certain temperature. As the temperature increases, thermal oscillation, or entropy, competes with the ferromagnetic tendency for spins to align. When the temperature rises beyond a certain point, called the **Curie temperature**, there is a second-order phase transition and the system can no longer maintain a spontaneous magnetization, although it still responds Paramagnetically to an external field. Below that temperature, there is a spontaneous symmetry breaking and random domains form (in the absence of an external field). The Curie temperature itself is a critical point, where the magnetic susceptibility is theoretically infinite and, although there is no net magnetization.

2.2.3 Diamagnetic Materials

Diamagnetic material is a very weak form of magnetism that is only exhibited in the presence of an external magnetic field. It is the result of changes in the orbital motion of electrons due to the external magnetic field. The induced magnetic moment is very small and in a direction opposite to that of the applied field. When a diamagnetic material is placed between the poles of a strong electromagnet, diamagnetic materials are attracted towards regions where the magnetic field is weak. Diamagnetism is found in all materials; however, because it is so weak it can only be observed in materials that do not exhibit other forms of magnetism. Also, diamagnetism is found in elements with paired electrons. Diamagnetic materials have a relative magnetic permeability that is less than 1, and a magnetic susceptibility that is less than 0. **Permeability** is the degree of magnetization of a material that responds linearly to a magnetic field. Magnetic permeability is represented by the symbol μ. Permeability in linear materials owes its existence to the approximation:

$$M = \chi_m H$$

where χ_m is a dimensionless scalar called the magnetic susceptibility according to the definition of the auxiliary field.

2.3 Perfect Diamagnetism (Meissner Effect)

Superconductors have unique combination of electric and magnetic properties. Although the term “superconducting” implies zero resistance, superconductors do not simply behave as perfect conductors (R = 0). In a perfect conductor the resistance around an imaginary close path is zero, therefore the amount of magnetic flux enclosed within this path cannot change. This must be true for any such imaginary circuit, which may happen only if the flux density at every point in the perfect conductor does not vary with time,

$$\frac{dB}{dt} = 0 \quad . \tag{2.1}$$

This means that if a perfect conductor at room temperature with no applied magnetic field is cooled to a very low temperature, and then a magnetic field is applied, the magnetic flux will not be allowed to enter the specimen and the interior will remain flux-free, since ***dB/dt***=0 must hold.

On the contrary, if a perfect conductor is subjected to an applied field before the cooling, the flux density inside will be the same as that of the external field. This is due to the value of the relative magnetic permeability in most metals, which is very close to unity, except for the ferromagnetic materials. If the metal is then cooled down to a low temperature, this will have no effect on the magnetization, and the flux distribution will remain unchanged. Now, as the applied field is removed, **dB/dt** must hold again, so that currents will be induced in the interior of the perfect conductor, maintaining the flux inside unchanged, (see Figure. 2.1 a).

In 1933, Meissner and Ochsenfeld measured the flux distribution of metal superconductors, cooled down to their T_c while in a magnetic field. They found out that a metal in the superconducting state never allows a magnetic flux density to exist in its interior. It exhibits perfect diamagnetism and the following equality always holds:

$$B = 0$$

This property, which cannot be explained by an equivalence of superconductors with perfect conductors, has been named **Meissner effect**.

The expulsion of an applied field is a result of the existence of induced currents in a superconductor, which generate magnetic field, opposite in direction and equal in magnitude to the external field, so that the total field inside the superconductor is zero. The cancellation of flux lines within the superconductor may be viewed as if the external field lines are 'forced' to circumvent the specimen and not allowed to enter inside. The pattern of the external field depends on the shape of the specimen and is characterized by the *demagnetizing factor* η of the geometry. For superconductors of slab geometry in parallel field (thin rectangle with infinite length) the demagnetizing factor is zero. For a cylinder in transversal field, η is 1/2, (see Figure. 2.2); for a sphere it is 1/3, and for a strip (thin rectangle in field perpendicular to its long side) the demagnetizing factor is nearly 1 (exactly 1 in case of infinite width of the strip). The state of perfect diamagnetism is retained only if the temperature is below T_c and the magnetic field below H.

2.4 Type-I Superconductors

Certain metals, such as titanium, aluminum, tin, mercury, lead, and others become superconducting. Their electric resistance completely disappears when they are cooled below their critical temperature. These metals were the first superconductors to be discovered and have been later named *Type-I superconductors.*

It was discovered that superconductivity is destroyed. The metal becomes normal again, in the presence of certain magnetic field, which is referred to as the critical field H_c. The value of H_c is related thermodynamically to the free-energy difference between the normal and the superconducting state.

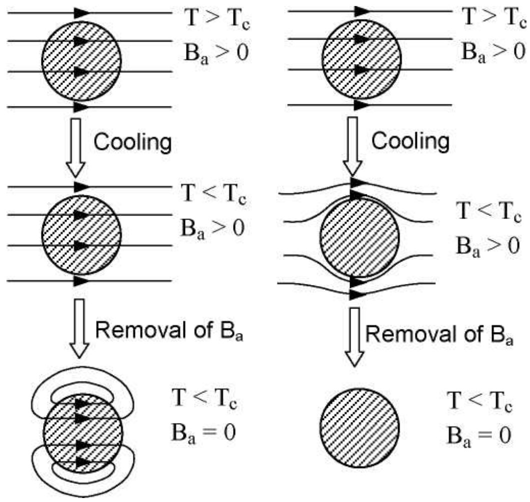

Figure 2.1 (a) in a perfect conductor the flux applied before the cooling is trapped so that $dB/dt = 0$ inside; (b) in a metal superconductor the flux is always expelled so that $B = 0$ inside (Meissner effect).

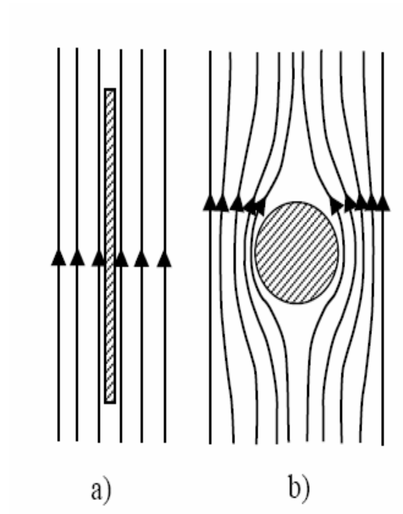

Figure 2.2 Pattern of the exterior field when demagnetizing factor is nearly zero for a slab of finite length (a) and when it is 1/2 for a cylinder in transverse field (b).

The critical temperatures, magnetic fields and magnetic flux densities of several Type-I superconductors are given in Table 2.2.

Table 2.2 Values of critical temperature, and critical magnetic field of same pure elements

Metal	*Tc(K)*	H_c *(A/m)*	B_c *(Tesla)*
Titanium (Ti)	0.4	$0.42\text{x}10^4$	0.0056
Aluminum (Al)	1.2	$0.79\text{x}10^4$	0.0105
Tin (Sn)	3.7	$2.40\text{x}10^4$	0.0305
Mercury (Hg) - α	4.2	$3.30\text{x}10^4$	0.0411
Lead (Pb)	7.2	$6.40\text{x}10^4$	0.0803

2.5 Type-II Superconductors

A significant contribution to the theory of superconductivity was made by Abrikosov in 1957 when he published a paper describing some new phenomena related to the Ginzburg-Landau theory, quite different from the behavior of the earlier Type-I superconductors [4]. He pointed out the existence of some new materials, which exhibited a continuous increase in flux penetration starting at a first critical field H_{c1} with reaching at a Second critical field H_{c2} (see figure 2.3) instead of showing a discontinuous disappearance of superconductivity at the thermo-dynamical field H_c. Later it was discovered that the behavior of these materials is not simply due to impurities in their chemical composition; they possessed entirely new properties and were termed thereafter *Type-II superconductors.*

While the class of Type-I superconductors is composed entirely of metallic chemical elements, Type-II superconductors may be metal alloys or even some pure metals, such as Niobium (Nb) and Vanadium (V), and also different oxide compounds. All metals and metal alloys which have their T_c below 30K and are referred to as *low temperature superconductors* (LTS), the oxide which superconductors have their T_c above 30K and are referred to as *high temperature superconductors* (HTS). Above H_{c2} there is no magnetization at all and the material returns to its normal state. As the magnetic field is decreased below H_{c2}, the reverse magnetization path will exactly retrace the forward one. However, no real material exhibits the exact retracing of the idealized curve. Structural imperfections or chemical impurities act as barriers for flux movement into the crystal; this is referred to as *flux pinning.* As a matter of fact, it is the practical goal of material engineers to introduce as many pinning sites as possible in order to allow high currents to flow under high magnetic fields. A real Type-II superconductor has more complicated magnetization path, which is depicted in Figure 2.3b. It is assume that H_a applied magnetic field strange

- $\boldsymbol{H_a < H_{c1}}$ applied field strength smaller than H_{c1}

Type-II superconductor behaves exactly like a Type-I superconductor and exhibiting a perfect diamagnetism and magnetization equal to $-H_a$

- $\boldsymbol{H_a = H_{c1}}$ the applied external magnetic field strength reaches H_{c1}

Normal cores with their associated vortices form at the surface and pass into material. The flux threading the vortices is in the same direction as that due to the applied magnetic field, so the flux in the material is no longer equal to zero and the magnitude of the magnetization suddenly decrease

- $\boldsymbol{H_{c1} < H_a < H_{c2}}$ the applied external field between H_{c1} and H_{c2}

In the field between H_{c1} and H_{c2} the number of vortices which occupy the sample is governed by the fact that vortices repel each other. The number of normal cores per unit area for given strength of applied magnetic field is such that there is equilibrium between the reduction free energy of material due to the presence of each non-diamagnetic core and the existence of mutual repulsion between the vortices. As the field strength of applied field is increased, the normal cores pack closer together, so the average flux density in the material increase and the magnitude of the magnetization decreases smoothly with increasing H_a. Near to upper critical field value H_{c2} the flux density and magnetization change linearly with applied field strength H_{c2} at the upper critical magnetic field.

- $\boldsymbol{H_a = H_{c2}}$ the applied external magnetic fields reach values of H_{c2}

There is a discontinuous change in the slope of the flux density and magnetization curve, and above H_{c2} the material is in the normal state with flux density equal to $\mu_0 H$ *and zero* magnetization

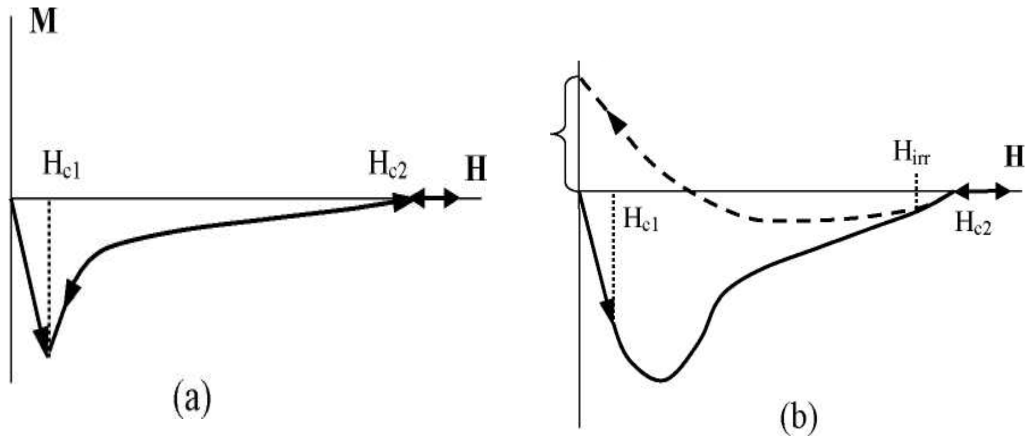

Figure 2.3 (a) Magnetization of ideal type-II superconductor. The state of perfect diamagnetism exists below H_{c1} and above H_{c2} the material is in normal state. (b) Magnetization of real type-II superconductor the curve is reversible only above H_{irr}. The magnetic flux at H = 0 is 'trapped' or 'pinned' in the material

2.6 The Mixed State

Apart from the normal and superconducting states, Type-II superconductors exhibit a new state, which is called the *mixed state,* which allows the existence of normal regions in the material. In the mixed state, Meissner effect is no longer present and magnetic flux may partially penetrate the superconductor; the superconductivity, however, is not lost. The existence of the mixed state can be explained by the fact that the material always tends to assume the state with lowest total free energy and when the surface energy between normal and superconducting regions is negative, the appearance of normal regions will reduce the total free energy and lead to a more favorable energy state [3]. It turns out that the configuration in which the ratio of surface to volume of normal material is a maximum is cylindrical normal regions, parallel to the external field and threading the superconductor, as shown in Figure 2.4. The cylindrical normal cores are arranged in a regular pattern, forming a lattice, sometimes called *fluxon lattice.* Within each core the magnetic flux has the same direction as that of the applied field and is shielded from the neighboring superconducting regions by a vortex of induced current. These supercurrents together with the surface current, circulating at the perimeter of the specimen, maintain the bulk diamagnetism, (see Figure 2.4). The mixed state is an intrinsic feature of Type-II superconductors and exists for magnetic fields such that $H_{c1} < H_a < H_{c2}$. It was predicted by Abrikosov that the magnetic flux would penetrate in a regular array of flux tubes, named fluxons, each one having the quantum of flux $\Phi_0 = h/2e$

Several years after Abrikosov, the magnetization of Type-II superconductors was experimentally described by Bean [5, 6]. He presented a macroscopic model of the current and magnetic flux distribution, and showed that the flux penetration in such materials is not uniform there is a flux density gradient and a flux-free region in the center of the specimen. Bean's model has been named the *critical state model* [7, 8]. Bean's model will be discussed in the next chapter.

2.7 Flux Pinning, Creep and Flow

In a perfectly pure material, the flux lines would be able to easily move and adjust their density according to the applied field. However, due to impurities and in homogeneities in Type-II superconductors, the fluxons are pinned and an energy barrier is created that has to be overcome in order to move them. Flux pinning can be imagined as if the fluxons are situated in pinning well of depth F_0 (pinning strength) and replace at a given distance, which fluxons need to jump to move from one well to another as shown in Figure 2.5

When electric current with density J is carried by a Type-II superconductor, it passes the flux lines and creates a Lorenz force $\boldsymbol{F_L} = \boldsymbol{J} \, x \, \boldsymbol{\Phi_0}$ upon each vortex. The fluxons will remain in place as long as their pinning strength F_0 is larger than the Lorenz force $\boldsymbol{F_L}$, even if the depth of the pinning wells is gets smaller with the increase of J. At a certain value J_c, the Lorentz force will become greater than the pinning strength, and all fluxons will start to move, (see Figure. 2.5). This movement is referred to *as flux-flow*. J_c is called the *critical current density* and is very important characteristic, since it gives the maximum current the superconductor can carry, and above which the material becomes normal again. In HTS, certain flux motion may be activated by thermal fluctuation of the fluxon lattice; this motion is slower and more sporadic and has been named *flux-creep.*

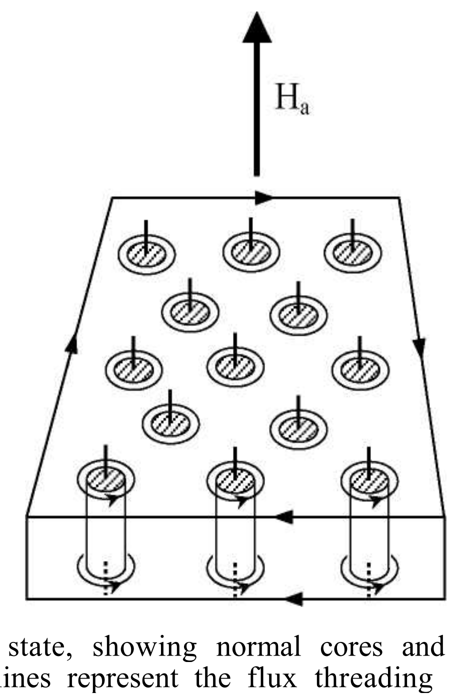

Figure 2.4The mixed state, showing normal cores and encircling supercurrent vortices. The vertical lines represent the flux threading the cores. The surface current maintains the bulk diamagnetism.

2.8 Lower and Upper Critical Fields

For Type-II superconductors, Abrikosov defined the relation of the lower (H_{c1}) and upper *(H_{c2})* critical field to the thermo dynamical critical field H_c as follows:

$$H_{c1} = {H_c}/{\kappa} \qquad\qquad H_{c2} = \sqrt{2}\kappa H_c$$

where κ is the Ginzburg-Landau constant of the material. It is equal to λ/ξ, where λ is penetration depth, at which the magnetic flux enters a superconducting specimen and ξ is the coherence length, which corresponds to the distance between the super electrons according to the Ginzburg-Landau theory the value of κ for Type-II superconductors can be experimentally obtained from the magnetization curves. For LTS materials it is usually between 4 and 34. κ is smaller than 0.71 surface energy positive for Type-I superconductor. κ is larger than 0.71 surface energy negative for Type-II superconductor.

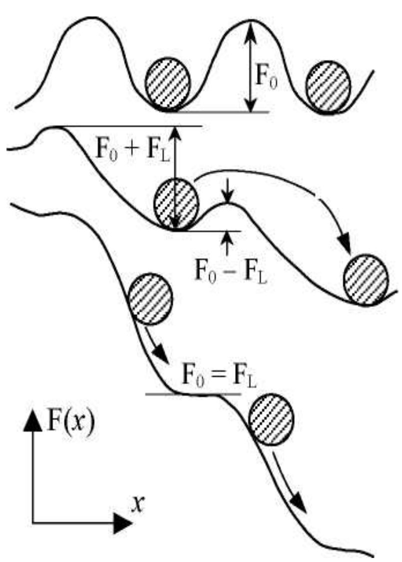

Figure 2.5 Mechanism of flux-flow. The presence of current in a magnetic field generates a Lorentz force, which tilts the staircase, allowing flux lines to hop out of their pinning wells more easily

The flux penetration *(B-H)* curves in Type-I and Type-II superconductors are depicted in Figure 2.6. Since the value of H_{c1} is very low, the approximation $B = \mu_0 H$ is often used for modeling purposes of Type-II superconductors.

TABLE 2-3 Values of Tc, H_{c2} and B_{c2} in same Type-II metal alloys superconductors

Compound	$T_c(K)$	H_{c2} *(A/m)*	B_{c2} *(Tesla)*
Nb-Ti alloy	10.2	~0.9xl0^7	- 12
Nb_3Sn	18.3	- 1.6x10'	~22
Nb_3Ge	23.0	~2.2xlO^7	~30
Nb_3Al	18.9	~2.3xlO^7	~32
$PbMo_6S_8$	14.0	-3.3x10'	~45

The values of H_{c2} and B_{c2} for several Type-II superconductors are given in Table 2.3. A great advantage of Type-II superconductors is the large magnetic fields, which they can support without losing their superconducting properties, compared to Type-I superconductors, for which the values of H_c are very low, see also Table 2.2

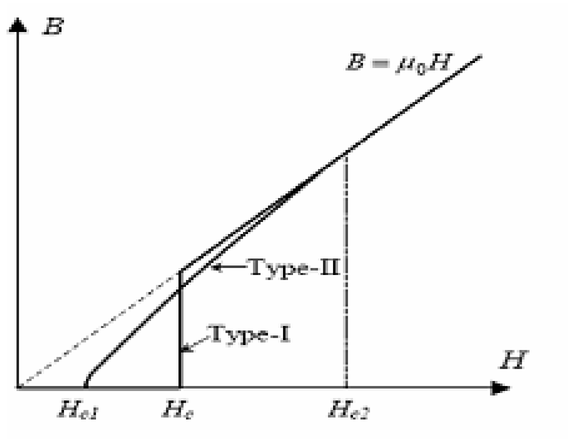

Figure 2.6 Comparison of flux penetration behaviors of Type-I and Type-II superconductors at same thermo dynamic critical field

CHAPTER 3

AC SUSCEPTIBILITY OF A SUPERCONDUCTOR AND BEAN MODEL

3.1 AC Susceptibility of a Superconductor

A magnetic material is described by its magnetization **M**(r), or magnetic dipole moment per unit volume at point's **r** throughout its volume.

Determining the magnetic field associated with an arbitrary magnetization distribution, **M**(r), can be difficult. However, if the material is in the shape of a long cylinder (solenoidal) and the magnetization is constant and points along the cylinder axis, the situation simplifies.

Before considering this special case, recall that for a long solenoid carrying a current I, the magnetic field outside the solenoid is zero and inside

$$B_{in} = \mu_0 nI \tag{3.1}$$

where n is the solenoid's number of turns per unit length. The field depends only on the product *nI* which can be called the current density and has SI units of A/m, the same as **M**.

The microscopic model for bulk magnetization is that it arises from the contributions of a great many atomic or molecular current loops. In the interior of the material, the current from adjacent loops are in opposite directions and these currents produce no magnetic field. On the material's boundary, however, the loop currents are unopposed, and lead to a surface current density (current per unit length) **M** x **n**, where n is the surface normal. For a constant axial magnetization **M** throughout a long, cylindrically shaped sample, the surface current density is constant and equal to **M**. This current circulates around the cylinder, like the current in a solenoid, and the magnetic field is the same as that of a solenoid with $nI = \boldsymbol{M}$, i.e. inside the material $B_{in} = \mu_0 M$ (a constant), and outside $B_{out} = 0$.

If such a sample is placed in a uniform magnetic field B_a oriented parallel to the sample axis, the net magnetic field is the superposition of the applied field and the field due to the magnetization. If the external field is written $B_a = \mu_0 M_a$, (which defines the magnetic intensity H_a) the magnetic field outside is just $B_{out} = \mu_0 M$ and the field inside becomes

$$B=\mu_0\left(H_a+M\right) \quad . \tag{3.2}$$

For some materials the magnetization is zero in the absence of an applied field and only becomes non-zero as a response to the applied field. For linear response materials, the magnetization will be aligned with (or against) the field and proportional to it. That is, we can write

$$M = \chi H_a \tag{3.3}$$

which define the material's susceptibility χ. Equation can then be expressed for paramagnetic materials, $\chi > 0$ and magnetic field is enhanced in the presence of the material. For diamagnetic materials, $\chi < 0$ and the field inside the material is reduced.

If the applied magnetic fields is not constant but is instead oscillating sinusoid ally along the sample axis at a frequency w

$$B = \mu_0 H_0 \cos wt \quad . \tag{3.4}$$

The general form for the magnetization is also sinusoidal at the frequency of the applied field, but it can be shifted in phase relative to the applied field. Relative to the applied field as given by Eq (3.4), the general form for the magnetization can be written

$$M(wt) = H_0(\chi' \cos wt + \chi'' \sin wt) \tag{3.5}$$

where χ' is real susceptibility of a sample and χ'' is imaginary susceptibility of a sample. It is important to remember that the product of an even and an odd function will be zero. Orthogonal condition it means that $\int \sin\Theta \cos\Theta d\Theta = 0$ it will be product $M(wt)$ with $\cos(wt)$ to obtain real susceptibility the χ' after that it will be product again $M(wt)$ with $\sin(wt)$ to obtain complex susceptibility χ''. After all of them we will integrate under exact a circle result of products so we can rewrite that

$$\chi' = \frac{1}{\pi B_a} \int_0^{2\pi} M(wt) \cos(wt) d(wt) \tag{3.6}$$

$$\chi'' = \frac{1}{\pi B_a} \int_0^{2\pi} M(wt)\sin(wt)d(wt) \tag{3.7}$$

These equations give us very important results. One of them gives us knowledge of internal structure of sample and if we look carefully to equation real and imaginary susceptibility related directly of magnetization of sample

For some materials, χ'' is nearly zero. If $\chi'' = 0$, the magnetization will be perfectly in phase with H_a for a paramagnetic material ($\chi' > 0$) and will be 180° out of phase for a diamagnetic material $\chi' < 0$ With nonzero values of χ'' , the magnetization given by Eq. (3.5) will be neither perfectly in phase nor out of phase with the applied field.

It turns out that only positive values of χ'' are physically possible (and thus that the magnetization can only lag the applied field). That only $\chi'' > 0$ is physically possible can be seen from the relationship between the sign of χ'' and the direction of energy flow between the sample and the applied field. The power density *P* (power per unit volume) absorbed in the sample is simply written

$$P = -M \frac{dB_a}{dt} \quad . \tag{3.8}$$

If some calculation will be making to obtain averaged value power density over a complete cycle as (remember that value of a sinus function over a complete cycle is equal to ½.

$$P_{av} = \frac{1}{2} \mu_0 w H_0^2 \chi'' \quad . \tag{3.9}$$

Only $P_{av} > 0$ $(\chi'' > 0)$ is energetically possible. In this case, the sample absorbs energy from the applied field that goes into heating the sample. Where $P_{av} < 0$

(χ''<0), rather than absorbing energy, the sample would be continually radiating energy a violation of the second law of thermodynamics. Non-linear magnetic materials in AC fields develop magnetization with higher harmonic components in addition to the fundamental expressed by Eq. (3.5). Thus, non-linear materials produce non-sinusoidal magnetization. We will emphasize the linear behavior. Self-induced flux of through the solenoid carrying a current I_s is defined by

$$\phi_s = NB_s A \tag{3.10}$$

where $N=nL$ total number of turns and $A = \pi R^2$ is the cross sectional area it can be written as

$$\phi_s = LI_s \tag{3.11}$$

where $L = \mu_0 n^2 V$ V is the solenoid volume and L is called the self inductance if a solenoid is placed with its axis along an applied field B_a flux through the solenoid due to applied field $\phi = NB_a A$ can be written

$$\phi_a = LI_a \ . \tag{3.12}$$

Magnetic flux of solenoid replacing in a magnetic field and where the pseudo-current I_a is defined by

$$I_a = \frac{B_a}{\mu_0 n} \ . \tag{3.13}$$

Thus, if the solenoid carries a current I_s the net flux through the solenoid can be expressed

$$\phi = L(I_s + I_a) \tag{3.14}$$

If the applied field B_a oscillates at a frequency w, ϕ_a will oscillate, and from Faraday's law of induction,

$$V = -\frac{d\phi}{dt} \tag{3.15}$$

An AC voltage will develop across the open solenoid ends. If a resistive load R is placed in series with the solenoid, an oscillating solenoid current I_s = V/R will develop, which then must be taken into account. If the magnetic field is given by Eq (3.4) and

$$I_s = {}^{H_0}\!/_{n}\left(\chi' \cos wt + \chi'' \sin wt\right) \qquad\qquad I_a = \frac{H_0}{n}\cos wt$$

where
$$\chi' = -\frac{w^2L^2}{R^2 + w^2L^2} \tag{3.16}$$

$$\chi'' = \frac{RwL}{R^2 + w^2L^2} \tag{3.17}$$

AC susceptibility is often known as the dynamic susceptibility. In this higher frequency case, the magnetization of the sample may lag behind the drive field, an effect that is detected by the magnetometer circuitry. Thus, the AC magnetic susceptibility measurement yields two quantities the magnitude of the susceptibility, χ and the phase shift, φ (relative to the drive signal). Alternately, one can think of the susceptibility as having an in-phase, or real, component χ' and an out-of-phase, or imaginary, component χ''. The two representations are related by

$$\begin{matrix} \chi' = \chi\cos\varphi \\ \chi'' = \chi\sin\varphi \end{matrix} \quad \Leftrightarrow \quad \chi^2 = \chi'^2 + \chi''^2$$

$$\chi = \sqrt{\chi'^2 + \chi''^2} \quad \Leftrightarrow \quad \begin{matrix} \chi = \chi' - i\chi'' \\ \chi = \chi' + i\chi'' \end{matrix}$$

$$\varphi = \arctan\left(\frac{\chi''}{\chi'}\right)$$

The real component χ' is just the slope of the ***M** (H)* curve discussed above. The imaginary component, χ'', indicates dissipative processes in the sample. In conductive samples, the dissipation is due to eddy currents. Also, both χ' and χ'' are very sensitive to thermodynamic phase changes, and are often used to measure transition temperatures. AC magnetometer allows one to probe all of these interesting phenomena. Typical measurements to access this information are χ vs. temperature, χ, driving frequency; AC susceptibility measurements $\chi = \chi' + i\chi''$ are very useful for characterizing the high temperature superconductors. The sharp decrease in the real part of $\chi'(T)$ below the critical temperature T_c is a manifestation of diamagnetic shielding and the peak in the imaginary part $\chi''(T)$ represent the AC loses. The shapes of $\chi'(T)$ and $\chi''(T)$ are strongly influenced by When we graph values of taking susceptibility dates the shapes of $\chi'(T)$ and $\chi''(T)$, are strongly influenced by [9]

i) The classes of compounds

ii) The fabrication process

iii) The thermal treatments

iv) The morphologies of the samples: bulk, thin film, wires , tapes , single crystals

v) The conditions of measurements (the presence and orientations of DC field along with AC field amplitudes

Many researchers have observed that complex AC susceptibility $\chi = \chi' + i\chi''$ of high *Tc* superconductors is weakly dependent on the frequency [10,11] (relative to field dependence) and it depend on strongly on the AC magnetic field amplitude.

3.2 The Critical State Model

Modelling tools for HTS superconductors are required since theoretical solutions for current and field equations have been found for simple geometries only and are based on the assumptions of Bean's critical state model, which is not fully applicable to superconductors with smooth current-voltage characteristics. In this thesis we used only slab geometry so we will explain theoretical background of Bean model for slab geometry.

A great advance in the theoretical modelling of superconductors was triggered in 1957 by a paper from Abrikosov [4], who presented a theory for the magnetization of hard (Type-II) superconductors, in which he showed that the flux enters the specimen in quantized flux lines, starting at very low field H_{c1} and completing its penetration at a much higher field H_{c2}. Several years afterwards, in order to obtain the virgin magnetization curves in hard superconductors, which exhibited magnetic hysteresis, Bean introduced a model, later referred to as the critical state model (CSM), a basic premise of which is the existence of a limiting macroscopic superconducting current density J_c that the superconductor can carry [5, 6]. In Bean's model only two states are possible to occur in the superconductor, zero current for regions with no magnetic flux penetration, and full current with density J_c in regions with partial or complete flux penetration.

Along the width of a superconducting specimen, the current density is given by

$$J(x) = \begin{cases} 0, & H(x) = 0 \\ \pm J_c & H(x) \neq 0 \end{cases} \tag{3.18}$$

In Maxwell's Equation, this can be also written as:

$$\nabla x B = \mu_0 J$$
$$\nabla x E = -\frac{\partial B}{\partial t} \tag{3.19}$$

with $J = \pm J_c$ or zero.

Even though experiments had shown that the critical current density is a function of the magnetic field, Bean assumed that J_c is independent of *B,* which in his early paper was equivalent to the assumption that the magnetic field is much less than the critical field of the filaments H_c.

3.2.1 Slab in a Parallel Field

Let us suppose the external field has amplitude H_a and increases. Following Lenz's law, screening currents will be induced at the edges of the slab. These induced currents will have direction such as to oppose the variation of the field and will try to screen the interior of the slab. Since the field has only y-component and the current flows in the z-direction, the curl of H in Ampere's law is reduced to one term. The field penetration profile is a straight line, whose slope is defined by J_c

$$\frac{\partial H_y}{\partial x} = \pm J_c \tag{3.20}$$

In this thesis we calculate theoretical critical current by using Bean model. According to this theory, critical current density as a function of the peak temperature (T_p) The critical current density at the peak temperature T_p, can be written [12]

$$J_c(T_p) = \frac{H^*}{a} \approx \frac{H^*}{\sqrt{ab}} \tag{3.21}$$

where the cross section of the rectangular bar shaped samples is $2a\ x\ 2b$ and a<b.

CHAPTER 4

EXPERIMENT

4.1 AC Susceptometer

The sample magnetization is studied using a conventional AC magnetic susceptometer. The susceptometer probe illustrated in Figure.4.1 includes a primary solenoid that produces a near-uniform AC magnetic field when driven by an AC source. Inside of primary coil is the secondary coil consisting of two pickup coils that are wound in opposite directions and electrically connected in series. The sample is placed in one of the pickup coil; the other one is left empty.

The AC voltage across the secondary coil is due to Faraday's Induction Law

$$V = -\frac{d\phi}{dt}$$

where Φ is the net flux through the entire secondary (both the sample and reference coil) and includes contributions from both the applied field and the field due to the sample magnetization.

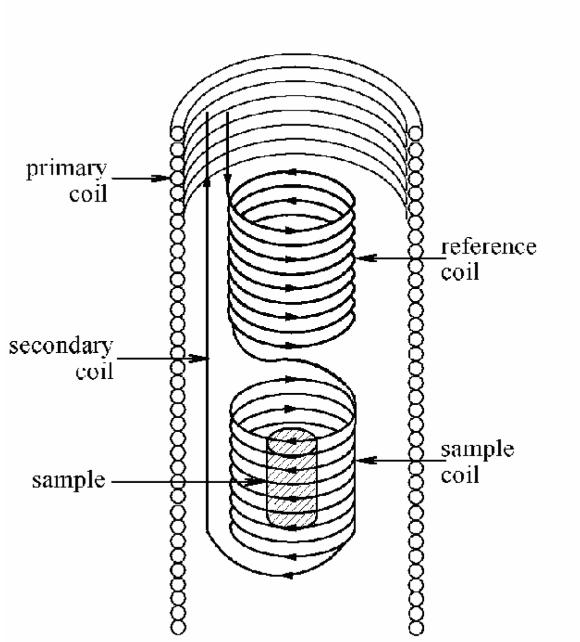

Figure 4.1 Primary and Secondary coil

Because the two pickup coils are wound in opposite direction and connected in series, the net secondary flux due to the applied field will be small. It is not exactly zero because of imperfections in probe construction, and thus, there is some small mismatch in the flux for the sample and reference coils. Of course, the net secondary flux due to the mismatch $\Phi_{mm,}$ will be proportional to primary field

$$\phi_{mm} = \alpha_{mm} B_a$$

α_{mm} is an effective mismatch area, which may be positive or negative depending on winding directions, and whether the sample or reference coil has the larger flux. Consequently, there will be some secondary signal $V = -d\phi_{mm}/dt$ (called the mismatch signal), which can be written as

$$V = V_{mm} \sin wt \tag{4.1}$$

where $V_{mm} = \alpha_{mm}\mu_0 wH_0$ gives the amplitude of the voltage due to mismatch. If a sample is present (in the sample coil) the magnetic field $\boldsymbol{\mu_0 M}$ associated with the induced magnetization will unbalance the fluxes in the sample and reference coil and there will be a large net flux Φ_m in the secondary. We could write

$$\phi_m = \alpha_m \mu_0 M$$

with the effective area $\alpha_{m.}$ Again, the sign of α_m depend on the winding directions. If **M** is given by Eq (3.5) there will be an induced secondary voltage

$$V = V_m(\chi' \sin wt - \chi'' \cos wt) \tag{4.2}$$

The net secondary voltage will include both sources Eq (4.1) and (4.2). In our application, two-phase lock in amplifier is used to measure both the amplitude of the secondary voltage and its phase (how much it lags or leads) relative to the monitor voltage. The lock-in amplifier takes the monitor voltage as the reference input, and it takes the secondary voltage as the signal input. Although the amplitude of the reference voltage is relatively unimportant, the origin of time is arbitrary, so the reference voltage can be expressed

$$V_r = V_{r0} \cos wt \tag{4.3}$$

Relative to this reference, an arbitrary signal voltage (at the same frequency) can be given by

$$V_s = V_{s0} \cos(wt - \delta) \tag{4.4}$$

where δ is the phase angle by which the signal lags the reference. Eq (4.4) can be written

$$V_s = V_x \cos wt + V_y \sin wt \tag{4.5}$$

where $V_x = V_{s0} \cos \delta$ and $V_y = V_{s0} \sin \delta$

The lock-in amplifier provides direct measurement of V_x and V_y (the lock-in out puts are actually rms value with signs i.e., $V_x/\sqrt{2}$ and $V_y/\sqrt{2}$ with a change of mode, the lock-in can also be made to provide $V_{s0}/\sqrt{2}$ and δ.)

Assuming that the monitor voltage (lock-in reference) is perfectly in phase with the primary field and that the secondary voltage is given by the sum of equation 4.1 and 4.2 the lock-in outputs are expected to be

$$V_x = -V_m \chi'' \tag{4.6}$$

$$V_y = V_{mm} + V_m \chi' \tag{4.7}$$

As can be see the outputs of lock-in is related to imaginary and real susceptibility so it can be accepted that behavior of the susceptibility is the same voltage output of lock-in so can be characterized magnetic behavior of any sample by using lock-in output

4.1.1 The Design of AC Susceptometer

AC susceptometer probe illustrated in Figure 4.2 and it includes a primary solenoid coil that produces a near-uniform AC source and the length of primary coil is 157 mm and the resistance of primary coil is 164Ώ. There are two secondary pickup coils that are wound in opposite direction and electrically connected in series inside of primary coil. One of pickup coils is named sample coil and the other one is reference coil. The primary and secondary coils are replaced inside a prexy tube as shown in Figure 4.2 and designed a heater to heat the from liquid nitrogen to room temperature system by wrapping nickel wire around of glass. It is used for heating susceptometer. In order to take low temperature the system is placed in a closed

Pyrex glass tube, which has electrical connection, temperature controller and thermocouple connection. There was another glass tube that includes all of heater, primary and secondary coils. A long rod is designed to move the superconductors into the coils. In order to measure precise temperature the thermocouple was mounted with vacuum grease tightly on the sample and thermocouple is attached on the sample.

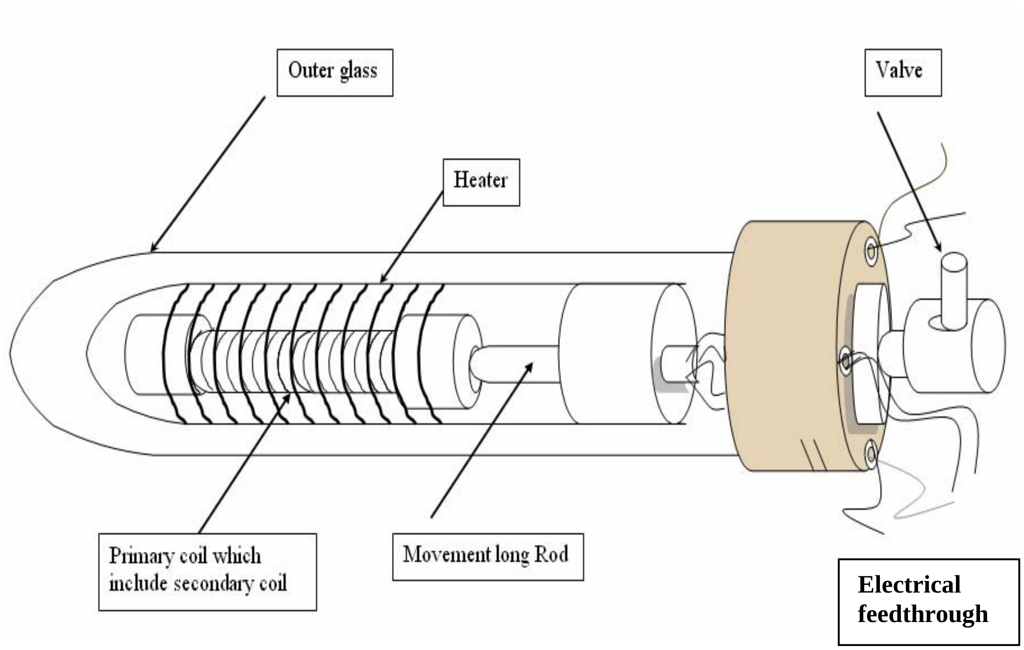

Figure 4.2 AC Susceptemeter

The valve is placed to the system to keep vacuum inside of Pyrex glass and to let Helium gas goes in shown in the Figure 4.2.

4.2 Thermocouple

In this experiment, copper and constantan used a thermocouple as a temperature sensor. The thermocouple is known *T* type thermocouple and it is used for low temperature measurement because this type of thermocouple works well at low temperature as shown in figure 4.3

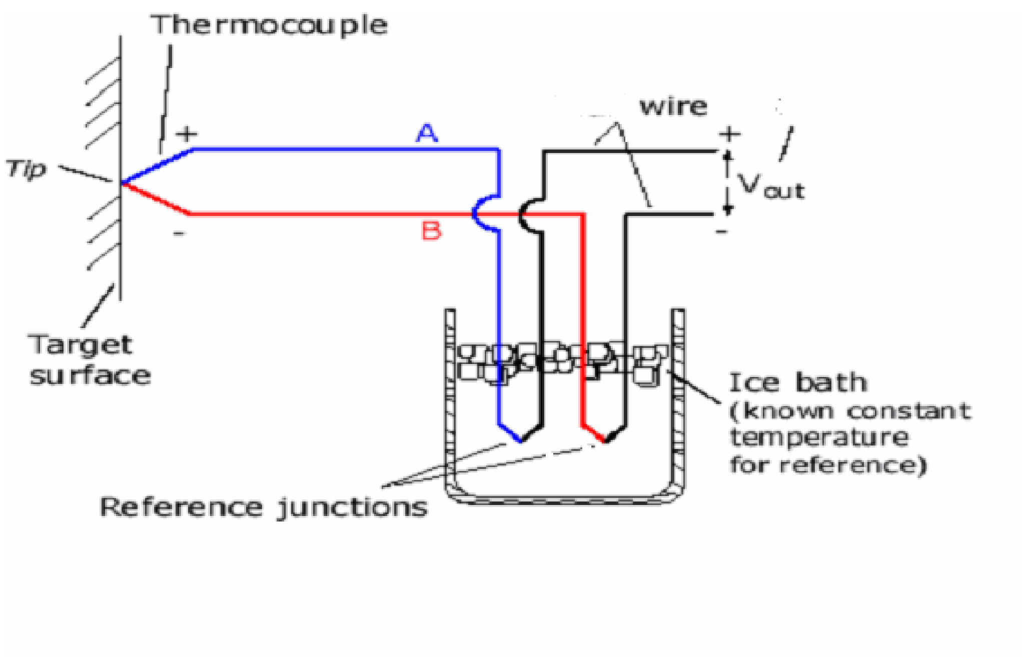

Figure 4.3 Typical Thermocouple Circuit

Thermocouples can create problems at the measurement of sample temperature. Some of them are

- All thermocouples have some mass. Heating this mass takes energy so will affect the temperature you are trying to measure.
- The output from a thermocouple is a small signal, so it is prone to electrical noise pick up. Most measuring instruments reject any common mode noise (signal that are the same on both wires) so noise can be minimized by twisting the cable together to help ensure both wires pick up the same noise.
- To minimize thermal shunting and improve response times, thermocouples are made of thin wire. This can cause the thermocouple to have a high

resistance which can make it sensitive to noise and can also cause errors due to the input impedance of the measuring instrument

- Another important point is that the mechanical contact of copper and constantan, it should be made very sensitive. If it is not well contact then thermocouple can create problem at the measurement of temperature.

4.3 Sample Preparation

Sm was substituted for the synthesis of $Bi_{1.6}Pb_{0.4}Sr_2Ca_{2-x}Sm_xCu_3O_y$ (x = 0.0, 0.0005, 0.001 and 0.005), the samples were prepared from Bi_2O_3, PbO, $SrCO_3$, CaO, Sm_2O_3 and CuO, taken in stoichiometric proportions by the standard solid-state reaction methods. The mixture was calcinated at the temperature 800 ºC for 24 h and the sample was reground, pressed into pellets 13 mm in diameter, then sintered at temperature 860 ºC for 200 h. The heating and cooling rates of the tube furnace for annealing were chosen to be 5 °C/min and 3 °C/min, respectively. After cooling to room temperature, the pellets were cut into rectangular bar shape (0.97 x 2.42 x 8.12 mm^3) for the AC susceptibility measurements.

4.4 Susceptibility Measurement

The AC susceptibility measurements on the samples were made using the homemade AC susceptometer. The lock-in Amplifier using in this experiment is Stanford Research SR850. In this work, we have four different Sm substitution samples to measure AC susceptibility. Firstly pure sample is placed on sample holder of long wood stick. Since it is used a grease to maintain thermal contact between thermocouple and sample. Vapour of water and some element of air freeze at 77K, it can obstruct taking our sensitive measurement and it can affect our system. For this reason, the air in Pyrex tube was evacuated. After vacuumed, helium gas was transferred into Pyrex glass to supply thermal contact with sample. Helium gas pressure was about 1 bar. Then Pyrex tube was dipped into liquid nitrogen bath. It took one and half-hour to reach the 77 K which is the temperature to begin AC susceptibility measurement. The AC field was applied along the longest dimension of the samples. The measurements started at 77 K with heating rate of 2 K/min in the temperature range 77 to 110 K at AC field amplitudes of 111, 222, 333, 444 and 555 A/m and 1 kHz of frequency. Data taken from Lock-in Amplifier were recorded using the Labview computer program. The samples are measured using the same method and analyzed. The obtained date is graphed by using Origin computer program.

CHAPTER 5

RESULTS AND DISCUSSION

5.1 Introduction

In order to investigate the magnetic properties of $Bi_{1.6}Pb_{0.4}Sr_2Ca_{2-x}Sm_xCu_3O_y$ (x=0, x=0.0005 x=0.001 x=0.005) samples AC susceptibility was carried out. Intergrain and intragrain effects due to Sm substitution are discussed. Intergrain critical current density is also calculated for different Sm substitution by using Bean Model.

5.2 AC Susceptibility

The real part of AC susceptibility of pure samples is normalized to -1. The real parts of susceptibility for the sample start to drop down at $\boldsymbol{T_{os}}$=101 K (it is named as an onset of bulk superconductivity) with decreasing temperature for different AC magnetic field. It shown that above 98 K, behavior is field independent, while below 98 K the behavior field dependent as shown as shown Figure 5.1. Because the pure sample is starting to be a superconductor at 98K, the curves for real part under different magnetic field are shifting to left with increasing of the strength-applied field. Imaginary parts show peaks at 97, 96, 95, 94 and 93 K for the fields

111, 222, 333, 444 and 555 A/m, respectively. As can be seen from the Figure 5.1, peak temperature (***T_p***) shifts to left when the field amplitude increases. The shift may be attributed to strength pinning force. The weaker the pinning, the larger is the shift in the maximum of χ'' [12]. At the peak values of the imaginary part, AC field amplitude equals to the full flux penetration field, H_p. At large AC field amplitudes (typically greater then 400 A/m) two loss peaks are often found; a broad peak at low temperature (coupling losses) and a narrower peak (intrinsic losses) near T_c. The intrinsic losses peaks are not observed in our measurement. This may be due to small inter-granular potential, small grain size and no flux penetration into the grains of the sample [11, 13].

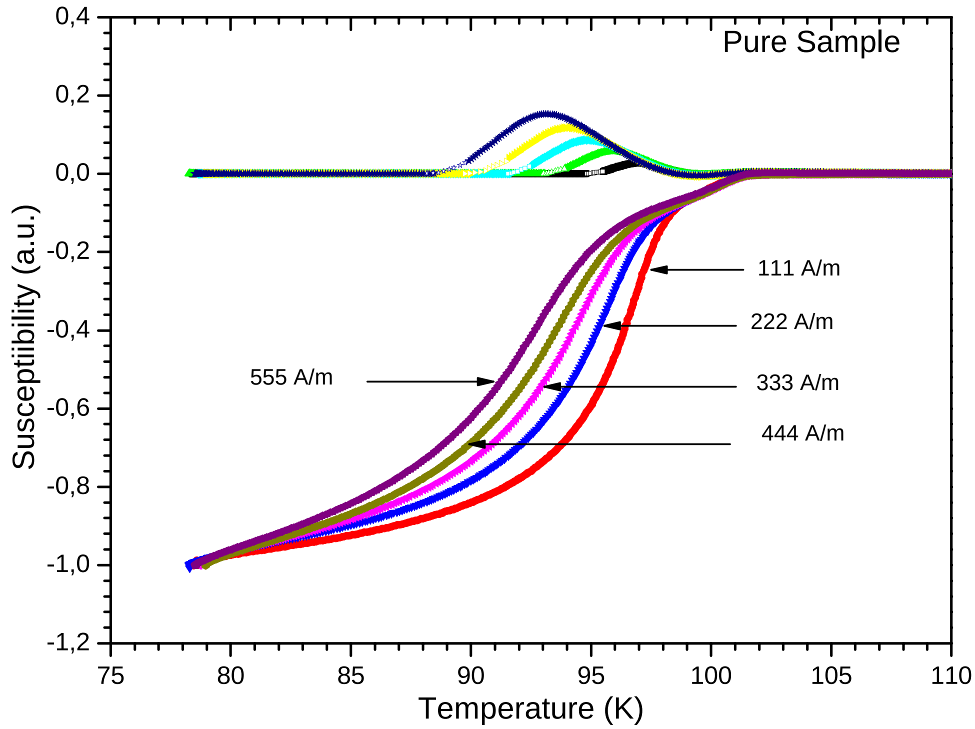

Figure 5.1 the AC susceptibility of ($\chi = \chi' + i\chi''$) versus temperature graphs for pure $Bi_{1.6}Pb_{0.4}Sr_2Ca_{2-x}Sm_xCu_3O_y$ sample with no Sm substitution

It can be seen in Figure 5.2-5.3-5.4 that Sm substitution shifts the susceptibility-temperature curves to lower temperature side and considerably increases the transition width in χ''-T curves and also decreases the shielding fraction of the superconducting phase in the samples. The broadening peak with increasing Sm substitution is due to gradual penetration of flux into the centre of the intergranular regions. The real and imaginary parts are zero ($\chi' = \chi'' = 0$) when the sample is in normal state (full penetration). χ'' goes to be positive due to extend of increasing flux penetration as the temperature shows slight decrease below T_{os}. At T_p, full penetration realized and peak reaches its maximum. Below T_p, the amplitude of χ'' falling due to decreasing amount of flux penetration. When the temperature reaches to lowest value ($\chi' = -1$ and χ''=0) the whole body starts to shield. This is apparent indication of the destructive effect in the superconducting properties brought about by Sm-Ca replacement in the Bi-2223 system. This is agreed with previous works [15, 16].

As can be seen in Figure 5.3 the onset temperature value of the sample with x=0.001 Sm substitution is at 98K. And again, this sample doesn't display an intrinsic peak at its imaginary susceptibility but the coupling loses are observed as we know the mechanism in superconductor material is micro bridge between grains [14].

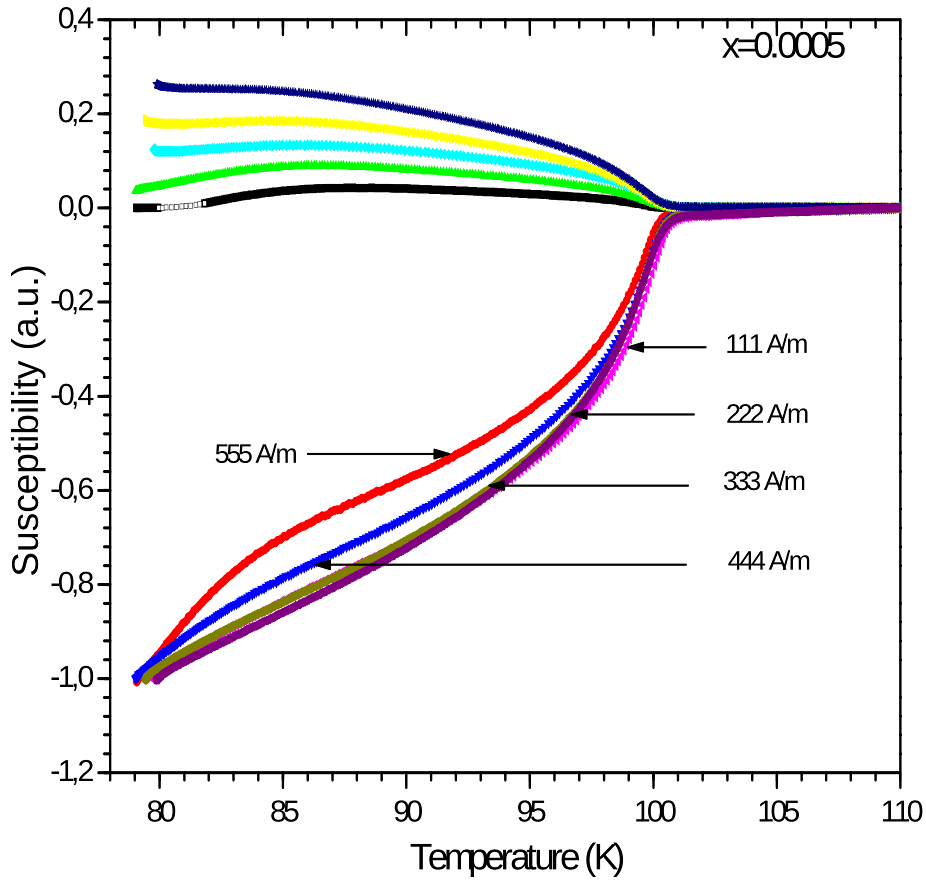

Figure 5.2 the AC susceptibility of ($\chi = \chi' + i\chi''$) versus temperature graphs for $Bi_{1.6}Pb_{0.4}Sr_2Ca_{2-x}Sm_xCu_3O_y$ sample with X=0.0005 Sm substitution

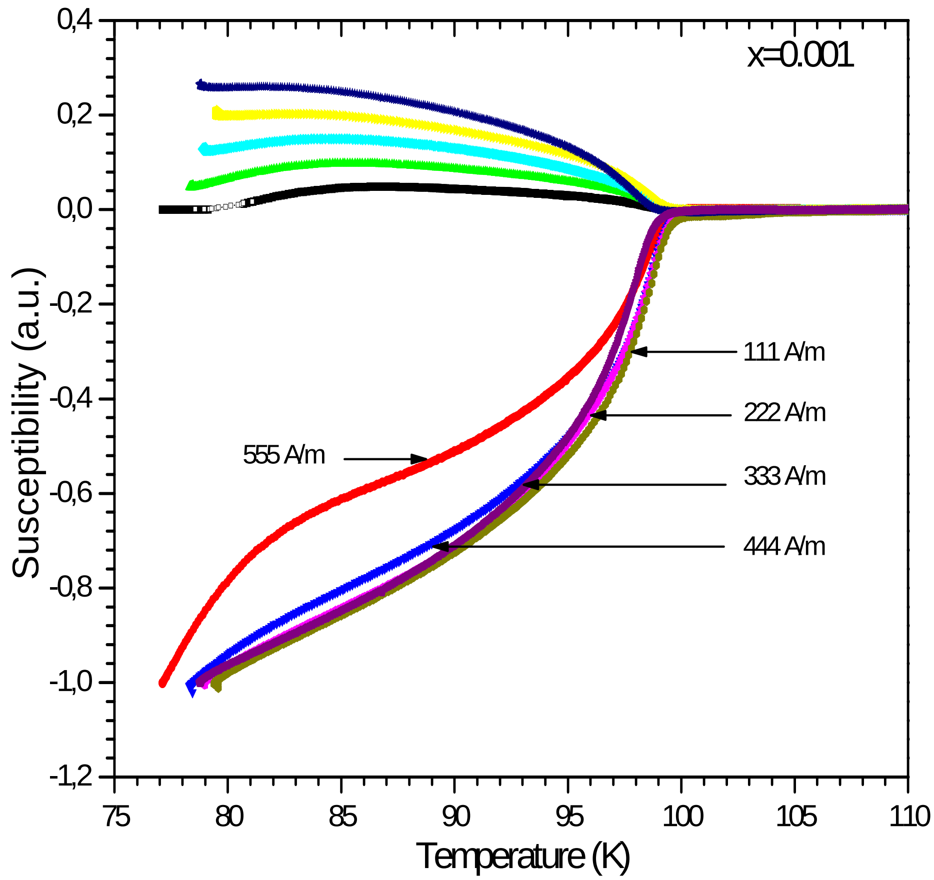

Figure 5.3 the AC susceptibility of ($\chi = \chi' + i\chi''$) versus temperature graphs for $Bi_{1.6}Pb_{0.4}Sr_2Ca_{2-x}Sm_xCu_3O_y$ sample with X=0.001 Sm substitution

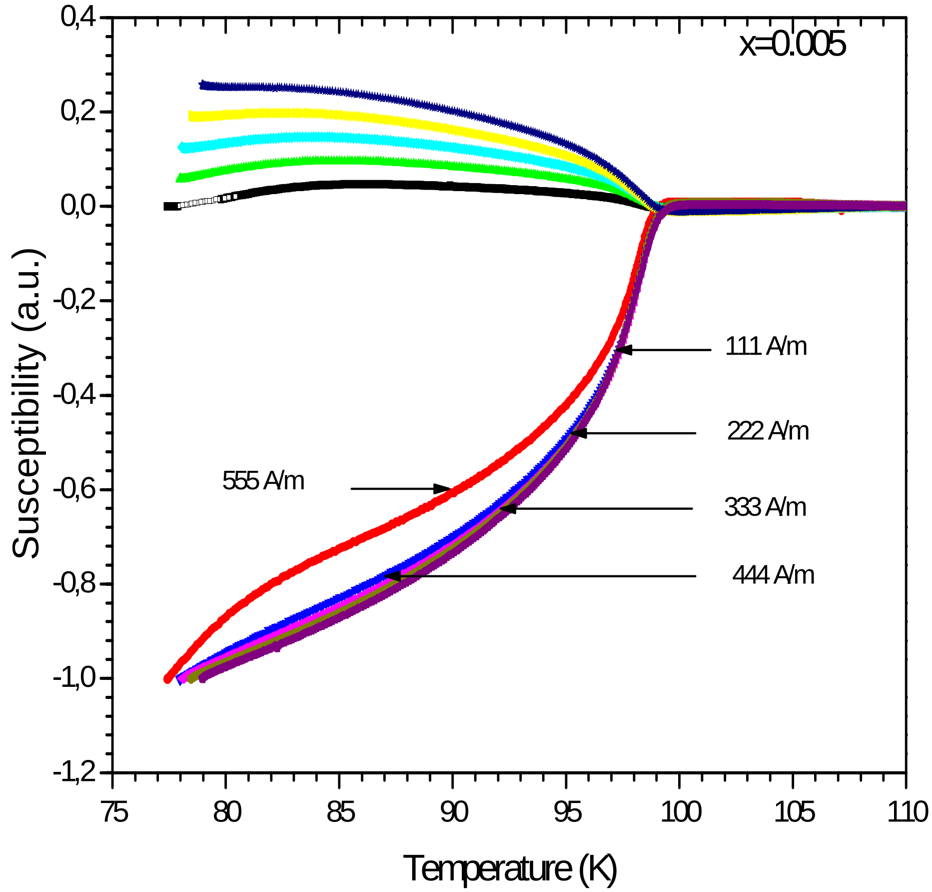

Figure 5.4 The AC susceptibility of ($\chi = \chi' + i\chi''$) versus temperature graphs for $Bi_{1.6}Pb_{0.4}Sr_2Ca_{2-x}Sm_xCu_3O_y$ sample with x=0.005 Sm substitution

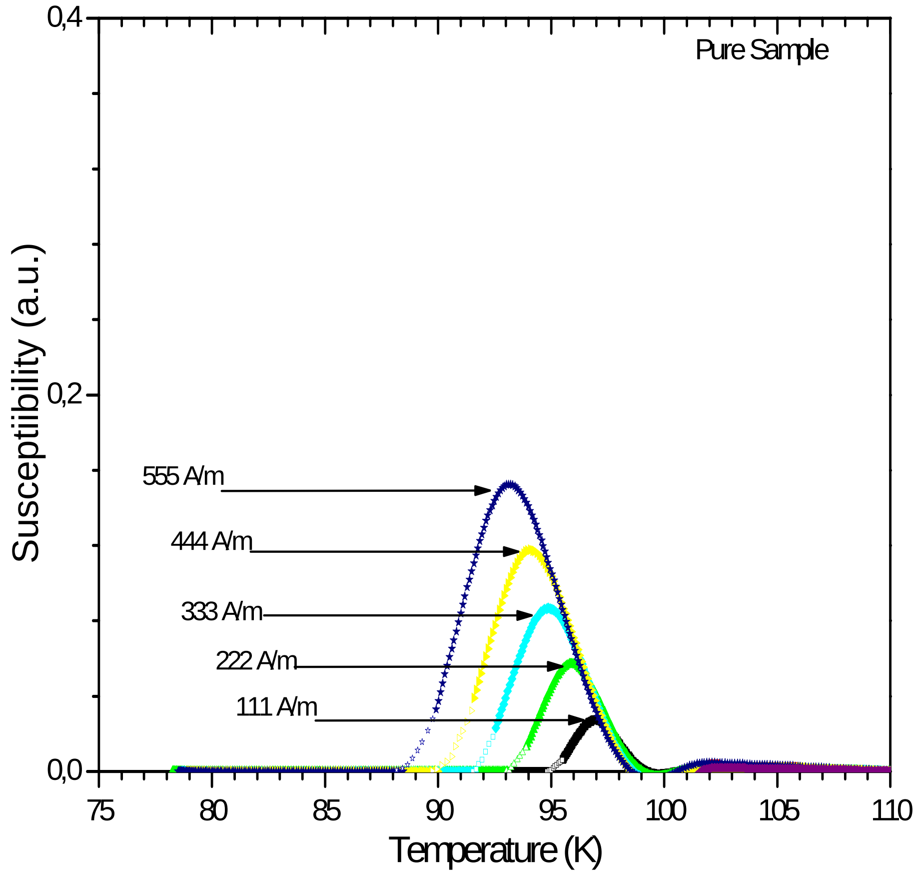

Figure 5.5 the imaginary part of AC susceptibility of χ'' versus temperature graphs for $Bi_{1.6}Pb_{0.4}Sr_2Ca_{2-x}Sm_xCu_3O_y$ sample for pure sample

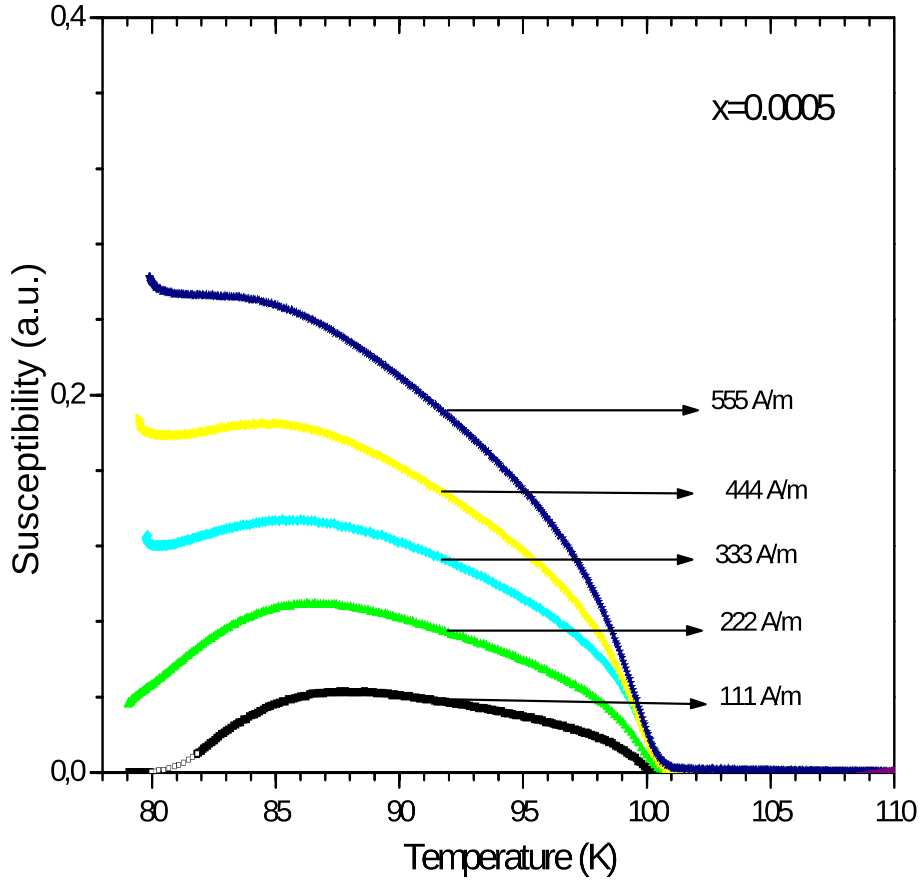

Figure 5.6 the imaginary part of AC susceptibility of χ'' versus temperature graphs for $Bi_{1.6}Pb_{0.4}Sr_2Ca_{2-x}Sm_xCu_3O_y$ sample with x=0.0005 Sm substitution

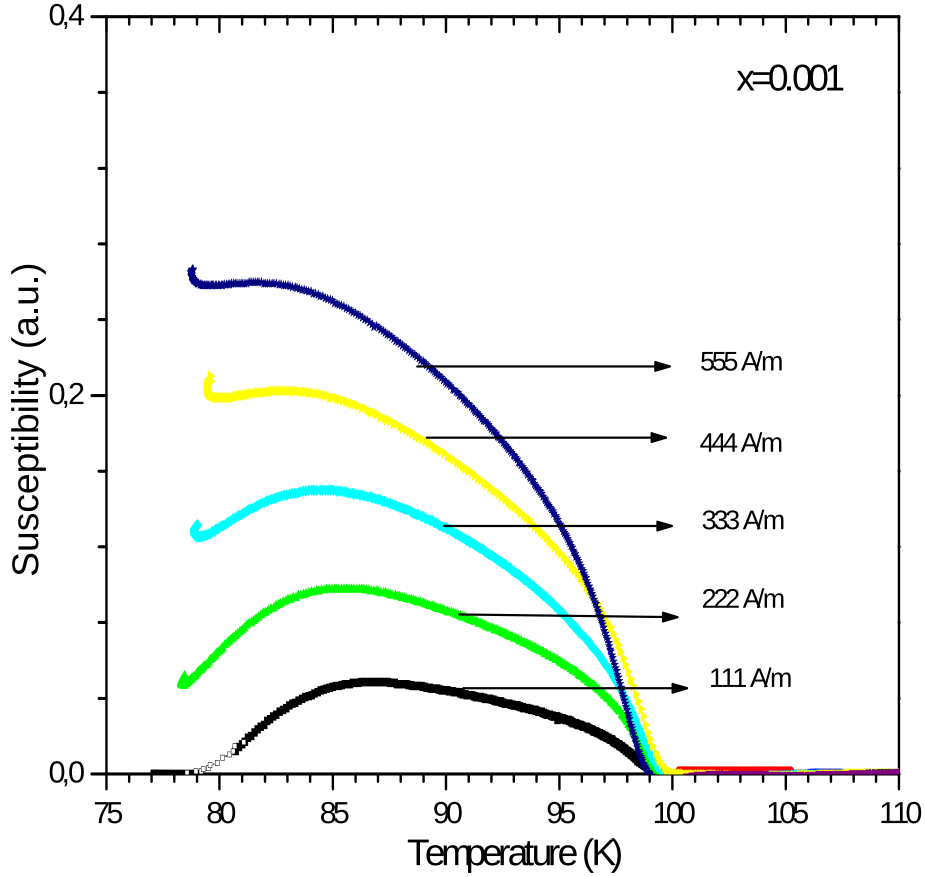

Figure 5.7 the imaginary part of AC susceptibility of χ'' versus temperature graphs for $Bi_{1.6}Pb_{0.4}Sr_2Ca_{2-x}Sm_xCu_3O_y$ sample with x=0.001 Sm substitution

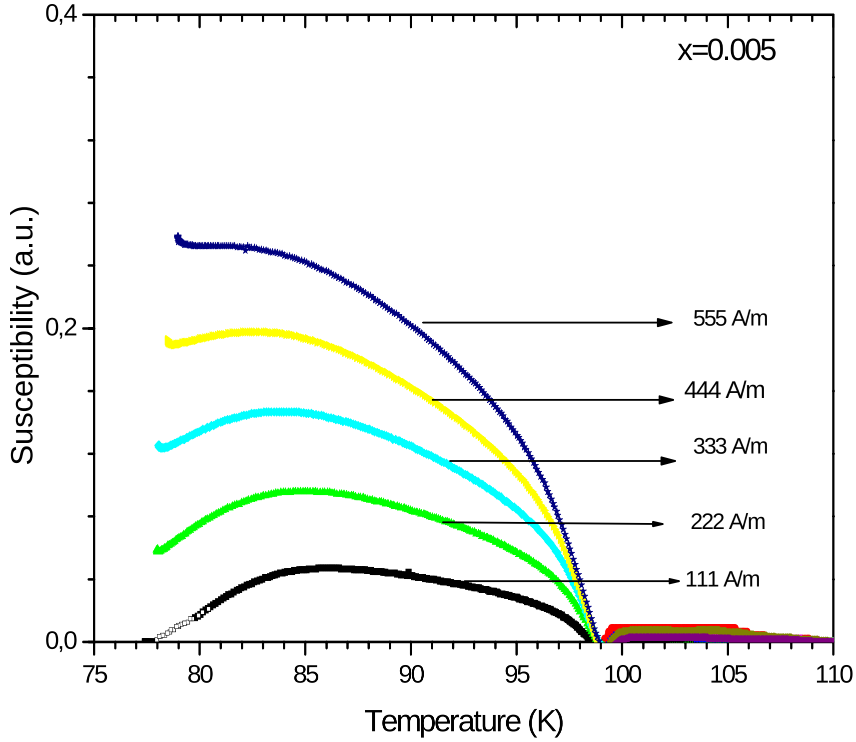

Figure 5.8 the imaginary part of AC susceptibility of χ'' versus temperature graphs for $Bi_{1.6}Pb_{0.4}Sr_2Ca_{2-x}Sm_xCu_3O_y$ sample with x=0.005 Sm substitution

5.3 Intergrain Critical Current Calculation

Figure.5.9 exhibits the critical current density versus temperature for the pure and Sm substituted samples. As seen from the graph, critical current density is about 66 A/cm^2 for pure Bi(Pb)SrCaCuO sample at 95 K. At 85 K, the critical current density decreases as 35, 27 and 21 A/cm^2 for the samples with x = 0.0005, 0.001 and 0.005 respectively. This may be explained by increasing in superconducting anisotropy factor brought about by the Sm substitution in Bi(Pb)SrCaCuO system [14].

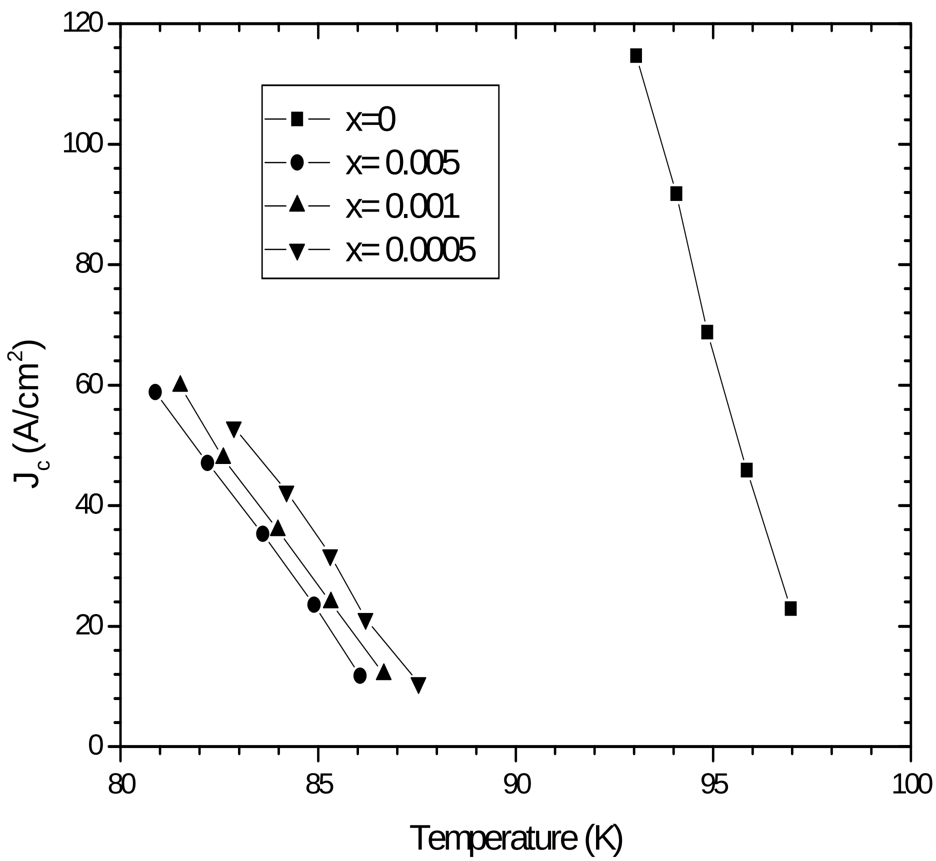

Figure 5.9 The critical current density versus temperature graph for the $Bi_{1.6}Pb_{0.4}Sr_2Ca_{2x}Sm_xCu_3O_y$ (x = 0, 0.0005, 0.001 and 0.005) samples. Solid lines are drawn for eye-guide only

5.4 Conclusion

In this thesis, Sm substitution effects, such as critical temperature, T_c, and critical current density, J_c, of $Bi_{1.6}Pb_{0.4}Sr_2Ca_{2-x}Sm_xCu_3O_y$ (x = 0.0, 0.0005, 0.001 and 0.005) was studied by AC magnetic susceptibility. The critical temperature of $Bi_{1.6}Pb_{0.4}Sr_2Ca_{2-x}Sm_xCu_3O_y$ was decreased by Sm substitution. The critical current density by Sm substitution in $Bi_{1.6}Pb_{0.4}Sr_2Ca_{2-x}Sm_xCu_3O_y$ is also decreased. The first (x=0.005) Sm substitution caused slight decrease in critical current density. Then critical current density decrease rate became lower. After First substation, it doesn't seem so very sharp a change while the amount of Sm substitution increases. This AC magnetic susceptibility method enabled us to investigate the magnetic behavior of the Sm substituted Bi(Pb)SrCaCuO superconductor sample. This method gives more intragrain date if the sample were powder. There are similar methods based this method, such as DC magnetic susceptibility and AC Hall prope method. Using those may give some different information about the sample.

REFERENCES

[1] H.K. Onnes, Further Experiments with Liquid Helium. On the Change of the Electrical Resistance of Pure Metal at Very Low Temperature, Leiden Comm. 122b (1911) 3-5.

[2] M.A. Omar, Elementary Solid State Physics: Principles and Applications, Addison-Wesley Publishing Company, Inc. New York November (1993).

[3] A.C. Rose-Innes and E.H Rhoderick, Introduction to Superconductivity, Oxford Pergaman Press London (1969).

[4] A.A. Abrikosov, On the Magnetic Properties of Supercondustors of the Second Group, J.Experim. Theoret. Phys. **32** (1957) 1442.

[5] C.P. Bean, Magnetization of Hard Superconductors, Phys. Rev. Letter. Phys. (1962) 250.

[6] C.P. Bean, Magnetization of High-Field Superconductors, Rev. Mod. Phys. (1964) 31.

[7] D. X. Chen, J. Nogues and K.V. Rao, AC Susceptibility and Intergranular Critical Current Density of High T_c Superconductors, Cryogenics **29** (1989) 800-808.

[8] F. Gomory and P. Lobotka, Determination of Shielding Current Density in Bulk Cylindrical Samples of High T_c Superconductors from AC Susceptibility Measurement, Solid State Commun. **66** (1988) 645.

[9] S. Çelebi, Comparative AC Susceptibility Analysis on Bi-(Pb)-Sr-Ca-Cu-O High-T_c Superconductors, Physica C **316** (1999) 251-256.

[10] S. Takacs and F. Gömery, Study of Flux Flow in High T_c Superconductors, Physica C **681** (1989) 162-164.

[11] M. Nikola and R.B. Goldfarb, Flux Creep and Activation Energies at the Grain Boundaries of Y-Ba-Cu-O Superconductors, Phys. Rev. B **39** (1989) 6615.

[12] S. Çelebi, I. Karaca, E. Aksu and A, Gencer, Frequency Dependence of the Intergranular AC Loss Peak in a High T_c Bi-(Pb)-Sr-Ca-Cu-O Bulk Superconductor, Physica C **309** (1998) 131-137.

[13] S. Çelebi, S. Nezir, A. Gencer, E. Yanmaz and M. Altunbaş, AC Losses and Irreversibility Line of Bi-(Pb)-Sr-Ca-Cu-O High-T_c Superconductors, Journal of Alloys and Compounds **255** (1997) 5-10.

[14] R.B Goldfard, M Leitental and C.A. Thomson, Alternating-Field Susceptometry and Magnetic Susceptibility of Superconductors, Magnetic Susceptibility of Superconductors and Other Spin Systems, Plenum Press New York (1992).

[15] A Coskun, A. Ekicibil, B. Ozcelik and K. Kiymac, Field Dependence of Magnetization and dM/dH for Sm- and Gd-Doped $Bi_{1.7}Pb_{0.3}Sr_2Ca_{2\_x}RE_xCu_3O_{10+y}$ Compounds, Chin. Phys. Lett. (2004) 21.

[16] S.K. Agarwal and B.V. Kumaraswamy, Low Field AC Susceptibility Study of Intergranular Critical Current Density in Mg-substituted $CuBa_2Ca_3Cu_4O_{12}K_y$ High Temperature Superconductors, Journal of Physics and Chemistry of Solids **66** (2005) 729-734.